

# Optical follow-up of ROSAT discovered candidate members of the open cluster Coma Berenices<sup>\*</sup>

R.J. García López<sup>1,2</sup>, S. Randich<sup>3</sup>, M.R. Zapatero Osorio<sup>1</sup>, and R. Pallavicini<sup>4</sup>

<sup>1</sup> Instituto de Astrofísica de Canarias, 38200 La Laguna, Tenerife, Spain (rgl@ll.iac.es; mosorio@ll.iac.es)

<sup>2</sup> Departamento de Astrofísica, Universidad de La Laguna, Avenida Astrofísico Francisco Sánchez s/n, 38071 La Laguna, Tenerife, Spain

<sup>3</sup> Osservatorio Astrofisico di Arcetri, Largo Fermi 5, 50125 Firenze, Italy (randich@arcetri.astro.it)

<sup>4</sup> Osservatorio Astronomico di Palermo, Piazza del Parlamento 1, 90134 Palermo, Italy (pallavic@oapa.astropa.unipa.it)

Received 24 March 2000 / Accepted 12 October 2000

**Abstract.** We have carried out an optical follow-up of twelve ROSAT discovered candidate members of the Coma Berenices open cluster. *VRI* photometry and low resolution ( $\sim 3 \text{ \AA}$ ) spectroscopy in the range 3800–7000 Å were performed to obtain colour-magnitude diagrams, proper motions, spectral types, chromospheric activity levels and radial velocities that allow us to establish whether or not these candidates are reliable cluster members. Only four of these objects show optical photometry marginally compatible with the main sequence delineated by known cluster stars. They also exhibit spectral types corresponding to late-K and early-M, and radial velocities which are not inconsistent with membership in Coma Berenices. The proper motions of these candidates are, however, very high and incompatible with the small value associated with the cluster. Thus, none of the ROSAT candidates can be considered members of Coma Berenices. This result tends to favour the hypothesis that the mass of the cluster and its average mass density are lower than what is required for stability, allowing the cluster dissolution by the escape of the less massive stars.

We discuss the probable nature of these objects on the basis of the available information. From our radial velocity observations we infer that five of them could be formed by multiple stars. In particular, we have discovered one W-type W UMa contact binary system (K6 spectral type) which is, in addition, a visual companion to a cooler star.

**Key words:** stars: activity – stars: binaries: eclipsing – stars: fundamental parameters – stars: late-type – Galaxy: open clusters and associations: individual: Coma Berenices – X-rays: stars

---

Send offprint requests to: R.J. García López

<sup>\*</sup> Based on observations made with the Isaac Newton telescope, operated on the island of La Palma by the Isaac Newton Group in the Spanish Observatorio del Roque de los Muchachos, with the IAC80 telescope and with the European Space Agency OGS telescope operated on the island of Tenerife by the Instituto de Astrofísica de Canarias in the Spanish Observatorio del Teide of the Instituto de Astrofísica de Canarias.

## 1. Introduction

ROSAT observations of several open stellar clusters have been carried out in the last few years with the primary purpose of studying the X-ray properties of their solar-type and low-mass members and investigating in detail their evolution with age and the age-rotation-activity connection (e.g., Randich 1997, 2000 and references therein; Jeffries 1999 and references therein). As a very important by-product, these X-ray surveys have allowed the identification of optically unknown low-mass candidate members of numerous clusters (e.g., Randich et al. 1995; Prosser et al. 1996; Randich et al. 1996a; Prosser & Randich 1998). As is well known, the level of X-ray activity decays, on average, with increasing stellar age and therefore low-mass stars in young clusters are expected to be vigorous X-ray emitters and they should be detected in sensitive enough X-ray surveys (Randich 1997; Jeffries 1999). As it is the case for X-ray selected T Tauri stars, optical photometric and spectroscopic follow-up observations are needed in order to investigate cluster membership and to infer at least the basic stellar properties (e.g., colours and spectral types) of the X-ray selected candidate members.

The open cluster in Coma Berenices (Cl Melotte 111) is known for its apparent deficit of low-mass stars. It has an estimated age  $\sim 400 - 600 \text{ Myr}$ , it is located at a distance of 86 pc (Van Leeuwen 1999), and its brightest stars are of A0 spectral type. Starting with the first proper motion/photometric/radial velocity survey of Coma (Trumpler 1938;  $v_{\text{rad}} = -0.4 \text{ km s}^{-1}$ ), different investigations have addressed the problem of the stellar population in this cluster (e.g., Artyukhina 1955; Argue & Kenworthy 1969; De Luca & Weis 1981; Bounatiro 1993); all the studies agreed in pointing out that the cluster has relatively few members (no more than 50–60) and, particularly, that the number of objects with  $V \geq 10.5$  (or  $M_V \geq 6$ , corresponding to  $\sim \text{KOV}$  spectral type) in the cluster is extremely small. De Luca & Weiss (1981) carried out *BVRI* photometry for 88 faint/red stars in the cluster region and concluded that the number of stars with  $10.5 < V < 15.5$  is probably not larger than 10. In other words, Coma Berenices appears to be generally poor in stars and, particularly, it is poor in low-mass stars.

According to both Trumpler (1938) and Argue & Kenworthy (1969), this result can be interpreted by assuming that the mass of the cluster and the average mass density are lower than what is required for stability, and therefore less massive cluster members could have escaped the cluster. Very recently Odenkirchen et al. (1998) analyzed astrometric and photometric data from the Hipparcos, Tycho, and ACT catalogs covering 1200 deg<sup>2</sup> around the center of Coma Berenices, and measured a radial velocity of  $-0.1 \pm 0.2$  km s<sup>-1</sup>; their primary aim was evidencing the process of escape and cluster dissolution by identifying cluster members in the surroundings of the cluster. They found that the cluster consists of a core and a halo extending up to  $\sim 5^\circ$  from the cluster center and of a moving group of extratidal stars, which witness the cluster dissolution. The luminosity function of stars in the core-halo region shows a steep decline beyond  $V = 10.5$ , while that of stars in the moving group continues to rise. They also found that faint stars are preferentially located at distances between  $3^\circ$  and  $4^\circ$  from the cluster center (but note that two of the faint stars from Artyukhina 1955 and Argue & Kenworthy 1969 are instead located very close to the cluster center).

Most of the optical searches for Coma Berenices members used proper motions as the prime criterion for selecting possible cluster candidates. However, there is one main difficulty in using proper motions for picking out possible Coma members: the cluster proper motion itself is very small (see section on proper motions). Odenkirchen et al. (1998) selected kinematic members on the basis of tangential space velocities, but as they point out, the sample suffers from incompleteness beyond  $V = 8.5$ . The question then arises whether the cluster is really poor in low-mass stars, or whether additional low-mass cluster members do exist, but have not been identified so far.

Randich et al. (1996b – hereafter RSP) carried out a ROSAT X-ray survey of Coma and found 12 X-ray sources that could not be identified with known Coma members, but that had an optical counterpart whose properties (namely, apparent visual magnitude, X-ray over optical flux, hardness ratio) were consistent with cluster membership. The sensitivity of the X-ray observations of Coma ranged between  $\log L_X \sim 27.9$  erg s<sup>-1</sup> and  $\log L_X \sim 29$  erg s<sup>-1</sup>, and the median X-ray luminosities of the K- and M-type dwarfs in the well studied Hyades open cluster are  $\log L_X = 28.41$  and  $28.21$  erg s<sup>-1</sup>, respectively (Pye et al. 1994). Under the assumption that the X-ray luminosity distribution function (XLDF) of Coma low-mass dwarfs does not significantly differ from the one of the Hyades, if a substantial number of K/M Coma members exists, the RSP X-ray survey should reveal at least part of them. If these 12 objects, or a fraction of them, turned out to be actual cluster members, there would be an indication that Coma Berenices' main-sequence does not virtually truncate around the K spectral-type and there would be an additional motivation to search for still unidentified faint, late-type Coma members. We carried out *VRI* photometry and low resolution spectroscopy in the visible for the X-ray cluster candidates in order to ascertain or reject membership for these objects and to infer their properties. The results of our optical follow-up are presented here.

**Table 1.** Coma Berenices candidate members.

#	ROSAT ID	$\alpha$ ( <sup>h</sup> <sup>m</sup> <sup>s</sup> )	$\delta$ ( <sup>°</sup> <sup>'</sup> <sup>''</sup> )	GSC name	V(GSC)
1a	RXJ 1212.0+2232	12 12 04.8	+22 32 01	1986.2106	11.6
2a	RXJ 1220.5+2648	12 20 34.3	+26 48 33	1991.1018	16.1
3	RXJ 1222.7+2711	12 22 47.6	+27 11 48	1991.0835	14.4
4	RXJ 1223.9+2245	12 23 55.0	+22 45 50	1989.0693	11.7
5	RXJ 1225.3+2220	12 25 19.0	+22 20 21	1447.1748	13.5
6	RXJ 1228.2+2549	12 28 12.5	+25 49 39	1989.2197	15.1
7	RXJ 1229.4+2259	12 29 26.7	+22 59 41	1989.2450	12.9
8	RXJ 1229.5+2711	12 29 33.6	+27 11 50	1991.0729	13.1
9	RXJ 1230.2+2518	12 30 14.0	+25 18 02	1989.2067	14.5
10	RXJ 1231.2+2348	12 31 14.0	+23 48 41	1989.2327	13.0
11	RXJ 1231.8+2847	12 31 48.3	+28 47 29	1991.1504	14.0
12	RXJ 1232.8+2750	12 32 52.9	+27 50 12	1991.1478	13.0

## 2. Observations

### 2.1. The sample

The target stars are listed in Table 1, where we basically repeat some of the information on the sources given by RSP; namely, we list a running number, the ROSAT ID RXJ number, the coordinates of the X-ray position, the HUBBLE *Guide Star Catalog* (GSC) number and V magnitude of the optical counterparts. We recall from RSP that none of the 12 X-ray sources had a counterpart in the SIMBAD catalog nor in any other catalogs available at the time apart from the GSC. Also note that, whereas RSP listed only one counterpart to the X-ray source #2 (since only one object is indeed listed in the GSC catalog), two very close objects are visible in the finding chart with an angular separation of  $\sim 13''$  (see Fig. 6 in RSP); we renamed them as objects #2a and #2b and observed both of them photometrically and spectroscopically. Within a distance of 2 arcmin from the star #1 there are two bright sources which will be also discussed later in this paper. They were measured as either secondary targets or for comparison purposes. This group of three stars will be referred to as #1a, #1b, and #1c (from brighter to fainter). We have obtained optical photometry for the three of them, but spectroscopy is available only for the X-ray candidate (#1a). In addition, the spectroscopy revealed that two of the objects (#6 and #9) were indeed AGNs, as confirmed by the Hamburg RASS Catalog of Opt. IDs (HRASSCAT; Bade et al. 1998) that became available after we had already carried out our observations. Although we have obtained photometry and spectroscopy for both objects, we obviously exclude them from the following discussion.

### 2.2. *VRI* photometry

CCD photometry in the Johnson *VRI* filters has been obtained for our target stars with the 0.8-m IAC80<sup>1</sup> telescope (Teide Observatory) on February 28, 1997. We used the Thomson (1024 × 1024 pixel) detector mounted at the Cassegrain focus

<sup>1</sup> IAC: Instituto de Astrofísica de Canarias

**Table 2.** Optical photometry, spectral types, H $\alpha$  equivalent widths, and estimated S (Ca II H&K) index (see Sects. 3.1 and 3.2).

#	$V$	$V - R$	$R - I$	$V - I$	SpT	EW* H $\alpha$ ( $\text{\AA}$ )	S
1a	$11.65 \pm 0.02$	$0.73 \pm 0.04$	$0.61 \pm 0.05$	$1.34 \pm 0.06$	K6 V (SB2)	$-0.7^{**} \pm 0.2$	$2.3^{**} \pm 0.5$
1b	$13.66 \pm 0.08$	$0.98 \pm 0.07$	$1.10 \pm 0.05$	$2.08 \pm 0.05$	–	–	–
1c	$16.13 \pm 0.08$	$0.98 \pm 0.13$	$1.22 \pm 0.10$	$2.20 \pm 0.15$	–	–	–
2a	$14.66 \pm 0.03$	$1.16 \pm 0.04$	$1.43 \pm 0.05$	$2.58 \pm 0.06$	M3.5 V	$-3.4 \pm 0.4$	$8.4 \pm 0.9$
2b	$15.77 \pm 0.05$	$0.70 \pm 0.06$	$0.68 \pm 0.05$	$1.38 \pm 0.06$	K6.5 V	$+0.6 \pm 0.2$	$1.6 \pm 0.3$
3	$13.78 \pm 0.03$	$1.06 \pm 0.04$	$1.28 \pm 0.05$	$2.34 \pm 0.06$	M2.5 V	$-3.9 \pm 0.4$	$7.8 \pm 0.8$
4	$11.91 \pm 0.02$	$0.46 \pm 0.04$	$0.43 \pm 0.05$	$0.88 \pm 0.06$	K0 V	$+1.1 \pm 0.5$	$0.9 \pm 0.2$
5	$13.68 \pm 0.03$	$0.36 \pm 0.04$	$0.32 \pm 0.05$	$0.68 \pm 0.06$	G6 V	$+3.2 \pm 0.5$	$0.2 \pm 0.1$
6	$16.66 \pm 0.08$	$0.40 \pm 0.09$	$0.47 \pm 0.08$	$0.88 \pm 0.09$	AGN	–	–
7	$14.14 \pm 0.03$	$1.17 \pm 0.04$	$1.49 \pm 0.05$	$2.66 \pm 0.06$	M3.5 V	$-2.2 \pm 0.4$	–
8	$13.08 \pm 0.02$	$0.34 \pm 0.04$	$0.34 \pm 0.05$	$0.68 \pm 0.06$	G7 V	$+2.8 \pm 0.5$	$0.2 \pm 0.1$
9	$15.19 \pm 0.05$	$0.38 \pm 0.06$	$0.49 \pm 0.06$	$0.63 \pm 0.07$	AGN	–	–
10	$13.98 \pm 0.03$	$0.74 \pm 0.04$	$0.68 \pm 0.05$	$1.42 \pm 0.06$	K6 V	$-2.0 \pm 0.4$	$3.3 \pm 0.4$
11	$14.03 \pm 0.03$	$0.60 \pm 0.04$	$0.50 \pm 0.05$	$1.10 \pm 0.06$	K3 V	$+1.0 \pm 0.5$	$0.4 \pm 0.1$
12	$13.22 \pm 0.02$	$0.50 \pm 0.04$	$0.48 \pm 0.05$	$0.98 \pm 0.06$	K1 V	$+0.0 \pm 0.5$	$1.3 \pm 0.2$

\* Positive EW values correspond to H $\alpha$  lines in absorption, negative values to H $\alpha$  emission.

\*\* These values are the average of six measurements. Their error bars also account for the observed variability. The complete lists are given in Table 5.

of the telescope, providing  $0''.43$ -sized pixels and a field of view of  $54.4 \text{ arcmin}^2$ . Exposure times were typically 30 s in all bands for the brighter stars and 60 s for the fainter ones. Raw frames were processed with usual techniques within the IRAF<sup>2</sup> environment, which included bias subtraction, flat-fielding and correction for bad pixels by interpolation with values from the nearest-neighbour pixels. We performed the aperture photometric analysis using routines within DAOPHOT and fixing circular apertures at 5–6 times the full width half maximum of each image (the seeing was stable around  $1''.5$  along the night). Instrumental magnitudes were corrected for atmospheric extinction and transformed into the  $VRI$  Cousins system using photometric standard stars from the Landolt (1992) list. Special care was taken in observing standards of different colours in order to ensure a reliable transformation for the reddest targets in our sample. Data were collected under photometric sky conditions resulting in small *rms* values for the final photometric calibrations (0.02, 0.03 and 0.04 mag for the  $V$ ,  $R$  and  $I$  filters, respectively). We present in Table 2 our measurements where  $1\sigma$  uncertainties in the  $V$  magnitude and colours account for the average *rms* of the calibration and the instrumental error as derived in IRAF. Fig. 1 illustrates the colour-magnitude diagrams for our data.

The star #1a (RXJ 1212.0+2232) turned out to be variable ( $\Delta \text{mag} \sim 0.8$ ) within intervals of minutes. We performed eight repeated observations of this star during the night of February 28; listed in Table 2 are the average magnitudes and colours determined that night. Unfortunately we cannot establish the possible photometric variable nature of the other star candidates (#2–12) in our sample because we obtained single exposures for

them. With the goal of deriving the period and amplitude of the light curve of the candidate #1a we re-observed it with the same instrumental setup at the IAC80 telescope on March 10, 1997, and using the Thomson CCD camera ( $1024 \times 1024$  pixel,  $0''.30$ -sized pixels and a field of view of  $26.2 \text{ arcmin}^2$ ) at the Cassegrain focus of the 1-m OGS<sup>3</sup> telescope (Teide Observatory) on April 19, 1999. Filters used were  $VI$  and only  $I$  for the IAC80 and OGS campaigns, respectively. Raw images were processed as previously described. We obtained relative aperture photometry between the target star and the two nearby, bright comparison stars (#1b and #1c) indicated in Fig. 2, and no photometric calibration has been evaluated for any of the nights. Exposure times were set so as to generally attain a count level for the variable star and the comparison stars which would enable photometric accuracies of 0.01 mag. Differencing the two comparisons confirmed that both stars were constant on the timescale of the observations and that the photometry had the desired accuracy. Consecutive images every 1.1 min during 7.4 hours were taken at the OGS telescope allowing us to measure a well-sampled light curve of the candidate. The nature of the star #1a will be discussed in Sect. 3.4.

### 2.3. Optical spectroscopy

Spectroscopic observations were carried out on March 14–16, 1997, with the Intermediate Dispersion Spectrograph at the Isaac Newton telescope (2.5m) in the Roque de los Muchachos Observatory (La Palma). Spectra were recorded using a  $1024 \times 1024$  pix ( $24 \mu\text{m}$ ) Tektronix CCD attached to the low resolution 235 mm camera. A window of 300 pix in the spatial direction was selected to match a slit length of  $39''$ . Two wavelength settings were used to cover from 3800 to 5500  $\text{\AA}$  (grat-

<sup>2</sup> IRAF is distributed by National Optical Astronomy Observatories, which is operated by the Association of Universities for Research in Astronomy, Inc., under contract with the National Science Foundation.

<sup>3</sup> OGS: Optical Ground Station of the European Space Agency

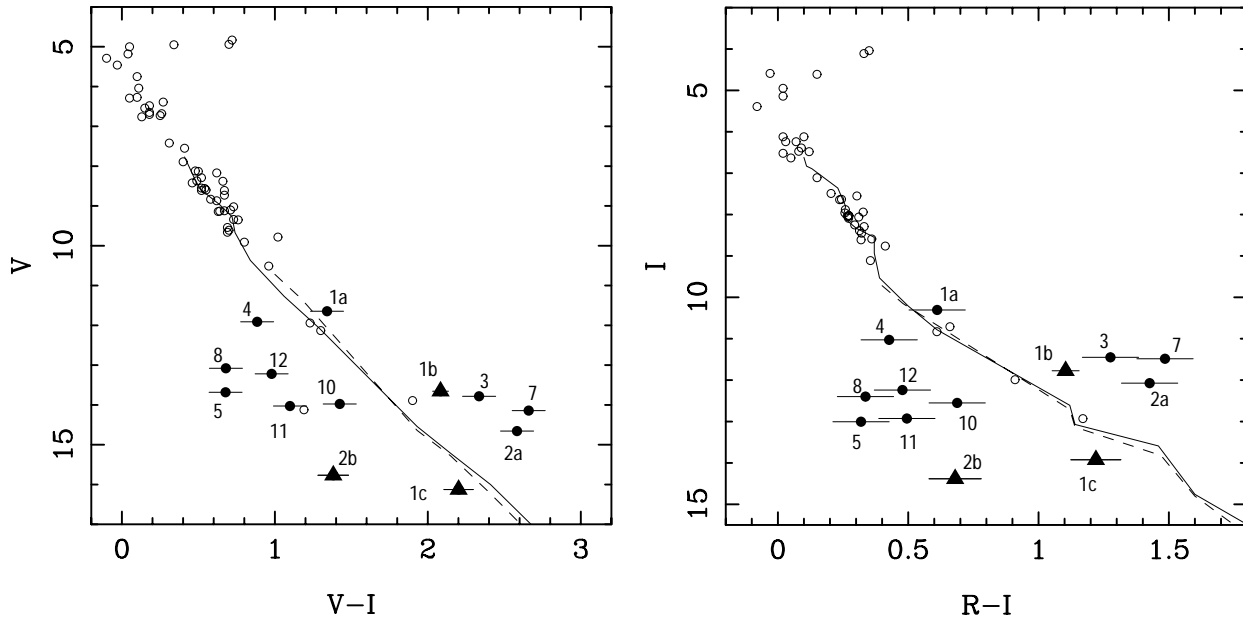


**Fig. 1.** Colour-magnitude diagrams for our targets (Cousins system). The stellar X-ray candidate members of the Coma Berenices cluster are indicated with filled circles, while three other stars also investigated in this paper are plotted with triangles. Objects are labelled as in the first column of Table 2. Error bars indicate  $2\sigma$  uncertainties in the photometry; errors in the y-axis are of the same size than the symbols. The cluster photometric sequence is given by previously known members represented with open circles in the figures. Overplotted to the data are the main sequence (solid line) from late-A to mid-M type field stars and the 600 Myr-isochrone (dashed line) by D’Antona & Mazzitelli (1998).

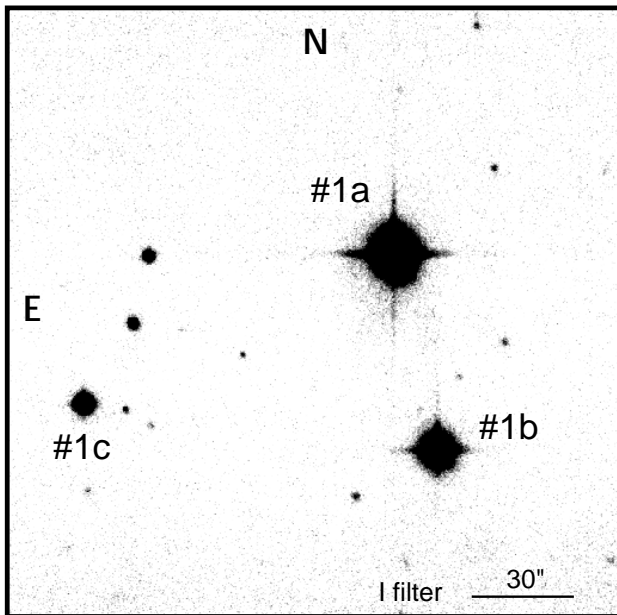


**Fig. 2.** Finding chart (*I*-band, OGS telescope) for the three stars studied in the field of the X-ray candidate #1a (RXJ 1212.0+2232). The three stars present high proper motion (not consistent with membership in the Coma Berenices cluster). Stars #1a (W-type WUMa binary) and #1b form a multiple stellar system.

ing R632V,  $\lambda_C = 4610 \text{ \AA}$ , slit width of  $1.6''$ ) and from 5300 to  $7000 \text{ \AA}$  (grating R600R,  $\lambda_C = 6144 \text{ \AA}$ , slit width of  $1.7''$ ), respectively, providing a spectral purity  $\sim 3 \text{ \AA}$  in both cases (corresponding to  $\lambda/\Delta\lambda \sim 1500$  and 2000).

Data reduction (bias subtraction, flat-field correction, sky subtraction, and extraction of one-dimensional spectra) was performed by standard procedures using routines included in the IRAF suite of programs. Wavelength calibration was carried out by comparison with exposures of CuAr and CuNe lamps obtained for the blue and red setups, respectively. Second-order polynomial fits were applied using 24 CuAr and 28 CuNe lines, providing a *rms* scatter  $\sim 0.1 \text{ \AA}$  in both cases, and final dispersions of  $1.6$  and  $1.7 \text{ \AA pix}^{-1}$ , respectively. The standard star Feige 66 (Oke 1990), observed under the same conditions, was used to correct for atmospheric extinction and the instrumental sensitivity along the spectral direction. Fig. 3 shows a sample of the final spectra for the 11 stars observed. They have been ordered from earlier to later spectral types (see Sect. 3.2). Blue and red spectra overlap smoothly in the  $5400 \text{ \AA}$  region, with the exception of the star #1a (K6V) for which the blue and red spectra shown correspond to different phases: 0.27 and 0.66, respectively. A detailed analysis of the spectroscopic properties of this sample will be presented in Sect. 3.2.

### 3. Analysis

#### 3.1. Colour-magnitude diagrams

In Fig. 1 we show the  $V$  vs  $V - I$  and  $I$  vs  $R - I$  colour-magnitude diagrams where we combine our photometric data of the X-ray candidates (filled circles) with magnitudes and colours from known Coma Berenices stellar members (open circles, Trumpler 1938; Artyukhina 1955; Argue & Kenworthy 1969; De Luca & Weiss 1981; Bounatiro 1993; Odenkirchen et al. 1998). Also included in the figure are the companion objects

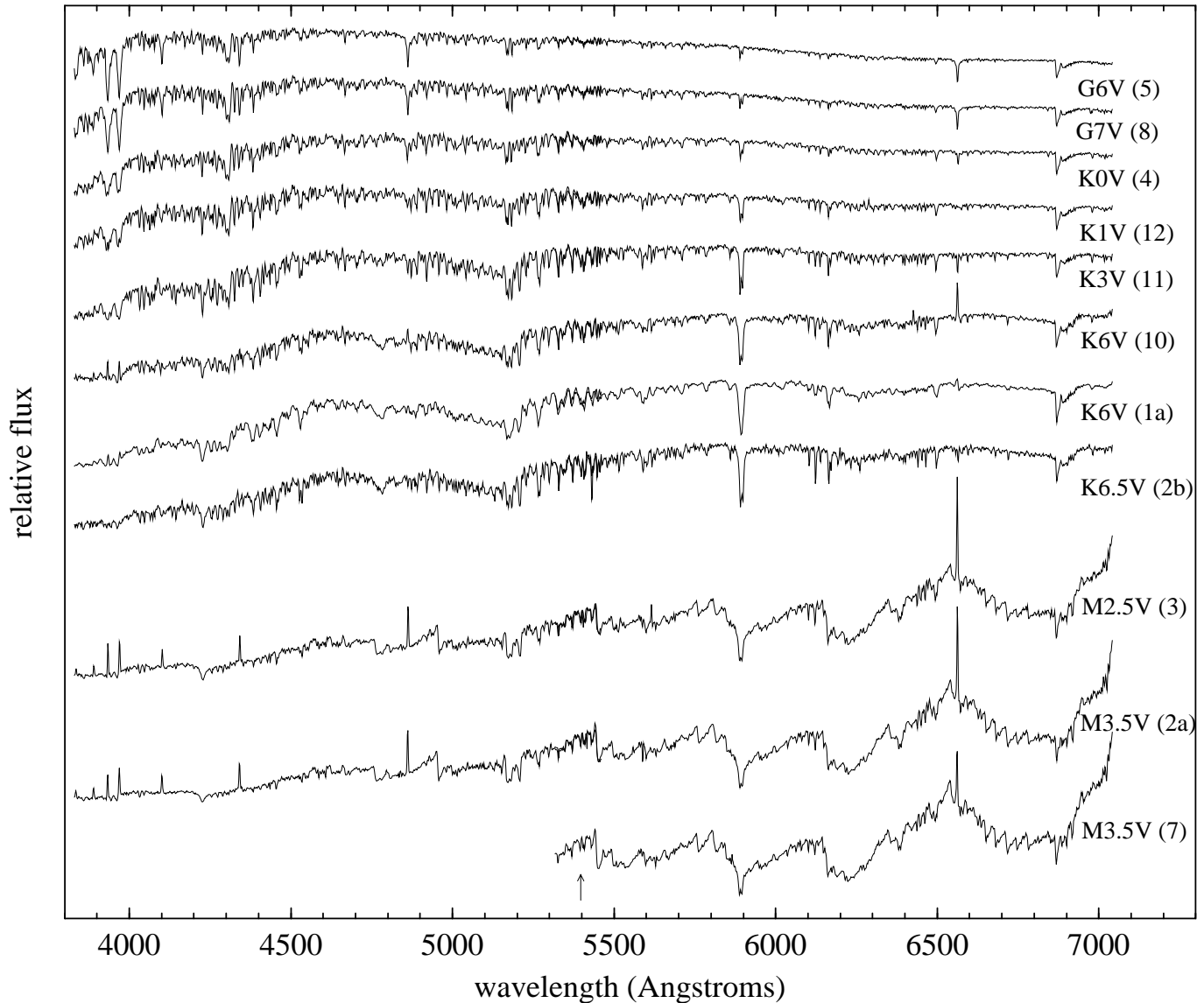


**Fig. 3.** Final spectra for the 11 stars observed. The spectra are ordered from earlier to later spectral types (see Sect. 3.2) and correspond, from top to bottom, to the following objects (indicated in parentheses): #5, #8, #4, #12, #11, #10, #1a, #2b, #3, #2a and #7. Blue and red spectra overlap smoothly in the 5400 Å region (indicated by an arrow), with the exception of the star #1a for which the blue and red spectra shown correspond to different phases.

#1b, #1c and #2b. *VRI* photometry for confirmed Trumpler’s Coma members have been adopted from Johnson & Knuckles (1955) and Mendoza (1963); we have taken the data for the remaining members from the SIMBAD and Hipparcos databases. Overplotted to the observations are the main sequence (solid line) for field stars and the 600 Myr-isochrone by D’Antona & Mazzitelli (1998, dashed line), both shifted to the distance of Coma Berenices ( $m - M = 4.77$ , Hipparcos). The main sequence for F-K spectral types have been taken from Pickles (1985), while that for the M-classes was derived from Leggett et al.’s (1996) paper. The theoretical isochrone ( $T_{\text{eff}}$ , luminosity) has been converted into the observables using the colour- $T_{\text{eff}}$  and colour- $BC(V)$  calibrations provided by Alonso et al. (1995, 1996) for the warmer stars and by Leggett et al. (1996)

for the cooler temperatures. Cluster members nicely fit both the main sequence and the 600 Myr-isochrone down to  $V, I = 14, 13$ , respectively. The age of 600 Myr has been recently suggested as the most likely age for the Coma Berenices stellar cluster (Odenkirchen et al. 1998).

A first glance at the two panels of Fig. 1 suggests that most of the candidates in our sample are likely to be Coma Berenices cluster non-members based on their photometry, and only one of them (#1a) plus stars #1b and #1c have a position not inconsistent with membership (considering  $3\sigma$  error bars). All the objects that we regard as non-members (#2b, #4, #5, #8, #10, #11 and #12) lie well below ( $\delta V, I \geq 1.5$  mag) the main sequence and the 600 Myr-isochrone and are considerably fainter than known Coma members with similar colours. Whereas non-

membership is easy to ascertain, it is more difficult to confirm membership. The star #1a (RXJ 1212.0+2232) lies very close both to the isochrone and the main sequence and to the position of two previously known members in the two diagrams, and thus it can be classified as a photometric member. The two other bright stars in the field (#1b and #1c) also show photometry marginally in agreement with the expected sequence for the cluster. On the contrary, the three coolest objects in our sample, #2a (RXJ 1220.5+2648), #3 (RXJ 1222.7+2711) and #7 (RXJ 1229.4+2259), are located considerably above the 600 Myr-isochrone by about 1.5–2 mag. The position of these stars is also inconsistent with that of two previously known members with similar magnitudes as it can be observed from the figure. However, these three stars could be younger than the mean age of the cluster (by a factor two – an age dispersion in the low-mass end of the Coma Berenices sequence cannot be ruled out), or could be binary systems, or could be a combination of both (X-ray surveys do present a clear bias in this respect toward young stars and close binary systems). Under these assumptions the location of each of the three stars in the colour-magnitude diagrams may well be explained. Thus, with photometry alone we cannot discard them as possible members of the Coma cluster. Proper motions and spectroscopy will allow us to unambiguously establish their membership status.

### 3.2. Spectral types, chromospheric activity and radial velocities

Spectral types are useful for studying cluster membership and estimating other stellar parameters (i.e., temperature, radius, and mass, etc.) which are utilized in detailed abundance studies or in interpreting additional data for these stars (e.g., X-ray fluxes, rotation periods, etc.). We have inferred the spectral types of our sample by comparing the spectra of the targets with those of spectroscopic standard stars both in the blue and in the red spectral ranges. Spectra of the following G5–M0-type standards (Jaschek 1978): HD 282025 (G5V), BD+43 2140 (G7V), HD 290982 (K0V), BD+35 2310 (K1V), BD–08 2823 (K3V), BD+17 2785 (K5V), BD+25 2874 (K7V) and BD+27 1311 (M0V), were obtained in the same run as for the program stars. For later spectral types we used data collected with the same instrumental setup in previous campaigns. In this case, only the red spectra have been considered for direct comparison between the target stars and the standards. We have derived the M spectral classification of the three coolest stars in our sample making use of molecular indices defined by Kirkpatrick et al. (1991) and Prosser et al. (1991). These indices are based on the relative strengths of CaH and TiO bands; TiO molecular absorptions dominate the optical energy distribution of the M-class objects. The Kirkpatrick et al.'s spectroscopic standards GL 338A (M0V), GL 767A (M1V), GL 767B (M2.5V), GL 569A (M3V), GL 402 (M4V) and GL 406 (M6V) have been used to transform Prosser et al.'s measured index values to a spectral type. A series of G5–M4III spectra were also available to us and we used them in order to investigate the luminosity class of the candidates. All of our stellar targets appear to be dwarfs rather than giants. We

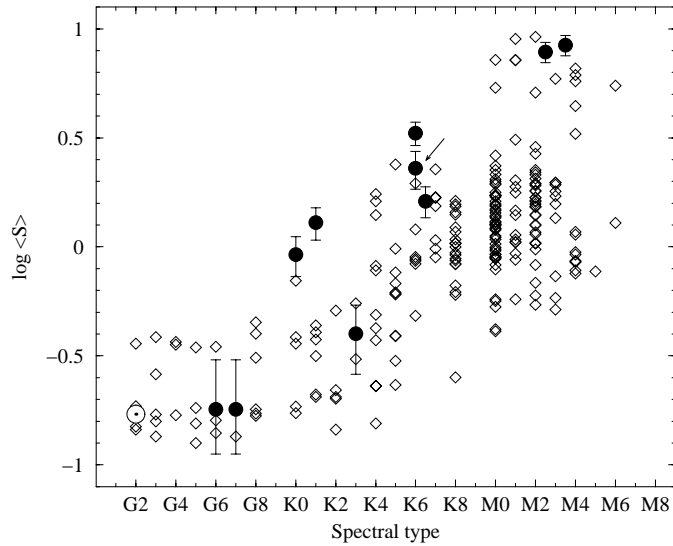
provide in Table 2 our determinations; the uncertainty in the K–M spectral classification is estimated at half a subclass. The final adopted spectral types are in the range G6V to M3.5V.

Fig. 3 shows clearly the changes in the spectral energy distribution for the stars of the sample. Photospheric Ca II H & K lines, which dominate at the earlier spectral types, progressively allow the appearance of the chromospheric components at the later types. The Na I D doublet at 5890 – 5896 Å increases with increasing spectral type, while H $\alpha$  changes accordingly from absorption to emission. In the spectrum of the star #12 (K1V) H $\alpha$  disappears in absorption as a result of a high chromospheric activity. This is consistent with the chromospheric emission observed at the bottom of the photospheric Ca II H & K lines in its spectrum. This is also the case for the star #10 (K6V), with both Ca II H & K and H $\alpha$  clearly in emission. Chromospheric activity appears to be also present in the star #4 (K0V). The spectrum presented in the figure for the star #1a (K6V) shows an inverse P-Cygni profile for H $\alpha$ . Changes from a P-Cygni profile to its inverse, passing through intermediate situations, were observed within periods of  $\sim 2$  hours. This behaviour is associated with the binary nature of this W-type W UMa object (see Sect. 3.4). Finally, it is seen how the spectra of the latest objects are mainly dominated by the presence of TiO bands.

In order to obtain a more quantitative evaluation of the chromospheric activity exhibited by the stars of this sample, we followed a similar procedure than that of García López et al. (1993) to estimate the S index for Ca II H & K lines (see Vaughan et al. 1978) from the observed spectra. We applied a numerical mask to our spectra, comprising two narrow bands of triangular profile centred on the H and K lines, and two square-topped broad bands, shifted to the red (R) and to the blue (V) of H and K, respectively. These bands were identical to the original bands defined by Vaughan et al. (1978) for their H-K photometer. An  $S'$  index was obtained by computing the following ratio between the equivalent widths measured for the chromospheric and continuum bands:  $S' = (H + K)/(V + R)$ . To convert our  $S'$  index to the original scale for the S index, we repeated this procedure for 15 dwarf stars with Ca II H&K spectra available in Montes et al. (1997), spectral types in the range G2V to K7V, and measurements of the S index listed in the catalogue of Duncan et al. (1991)<sup>4</sup>. Before applying the mask, the original spectra of these stars were degraded to match our lower spectral resolution. The resulting values, with the error bars associated with this procedure, are given in Table 2.

Fig. 4 shows the chromospheric activity estimated for our stars compared with the mean S values for a sample of measurements of G- to K-type stars from Noyes et al. (1984), complemented with mean values listed by Duncan et al. (1991) for M-type stars of the Woolley et al. (1970) catalogue of stars within 25 pc of the Sun. The compilation of comparison stars is

<sup>4</sup> The stars used were: HD 3651 (K0), HD 4628 (K2), HD 10476 (K1), HD 16160 (K3), HD 20630 (G5), HD 22049 (K2), HD 81809 (G2), HD 115404 (K3), HD 144287 (G8), HD 101501 (G8), HD 182488 (G8), HD 190404 (K1), HD 201091 (K5), HD 201092 (K7), and HD 219134 (K3). Their spectra are available at: <http://www.ucm.es/info/Astrof/fgkmsl/fgkmsl.html>



**Fig. 4.** Values of the S index estimated from the blue spectra of our sample stars (filled circles) vs. spectral type, compared with mean S values taken from the literature for late-type dwarfs (open diamonds), obtained using the H-K photometer (see text). The location of the Sun is shown with the usual symbol and the variable star RXJ 1212.0+2232 is indicated with an arrow. Note that the X-ray selected stars exhibit, in general, a very high level of chromospheric activity.

by no means exhaustive but provides a reference frame to evaluate the behaviour of the chromospheric activity of the X-ray selected stars. It can be seen how our stars with spectral type later than K0 are located in the upper part of the distribution, showing in general a high level of activity as it was expected from their high coronal emission. The previous qualitative considerations about the chromospheric activity of stars #4 (K0), #12 (K1) and #10 (K6) are clearly confirmed. The star #11 (K3) shows a lower level of activity but still much higher than other values observed for its spectral type. The error bar shown for the binary star #1a (indicated by an arrow) includes the variability observed for its chromospheric activity in six different measurements. The corresponding individual values are listed in Table 5. The two M-type stars of our sample with available blue spectra show a very high level of activity. This is not the case for the two G-type stars. The S values estimated for them are located in the lower strip of the distribution, below the so called “gap” of Vaughan & Preston (1980), which is believed to separate “old” and “young” G-type stars (Barry 1988), although it has also been ascribed to the combined action of two phenomena: the time-dependence of the stellar spin down and the colour-dependent shape of the activity-rotation relation for stars earlier than  $\sim$ K2 (Walter 1982; Rutten 1987). The error bars for these two stars allow them, however, to be potentially more active. This would be in better agreement with their coronal emission, for which we estimate a lower limit similar to those of the stars in the upper part of the distribution (and typically at least one order of magnitude larger than those of the stars in the lower part). It could also be possible that these stars are indeed quiescent and not the real optical counterparts to the

X-ray sources detected by ROSAT. The lower limit for their chromospheric activity is given by the minimum (basal) flux for their spectral type (Schrijver et al. 1989).

The spectral types that we derived for our sample stars are in full agreement with their colours, with the only marginal exception of the star #10 (K6V), whose spectrum appears to be slightly earlier than that of the star #2b (K6.5V) which shows slightly bluer colours but within the error bars. This general good agreement could be an indication that the extinction is low towards the direction of the sources. Using the spectral type-magnitude relationship defined by Coma Berenices members, only four objects in our sample (#1a, #2a, #3 and #7) fit the spectral sequence of the cluster. This result is very similar to that derived from the optical photometry. The seven remaining X-ray candidates appear to have low-luminosity for their spectral types, and thus, they are more distant than the cluster and are not members.

Due to the limited resolution of our spectra, we cannot infer radial velocities with a precision better than  $15\text{--}20\text{ km s}^{-1}$  and, therefore, we cannot definitively confirm membership using radial velocities. A mean radial velocity of about  $0\text{ km s}^{-1}$  has been inferred for Coma Berenices (see Trumpler 1938, who derived  $v_{\text{rad}} = -0.4\text{ km s}^{-1}$ ; Odenkirchen et al. 1998, who obtained  $v_{\text{rad}} = -0.1 \pm 0.2\text{ km s}^{-1}$ ). When we performed the spectroscopic observations we already knew that the star #1a showed photometric variability. Because of this, we obtained a number of spectra on this target in order to also detect radial velocity changes (see Sect. 3.4 for further details). For deriving radial velocities we have cross-correlated the spectra of our target stars with the spectra of two standard stars for which radial velocities are available to high degree of accuracy (HD 107513  $v_{\text{rad}} = -1.1\text{ km s}^{-1}$ , BD+17 2785  $v_{\text{rad}} = +45.7\text{ km s}^{-1}$ ; Dufflot et al. 1995). These data were obtained with the same instrumental setup during our spectroscopic campaign. Before deriving the radial velocities, all the spectra were set to a common origin by shifting sky lines to laboratory wavelengths. The cross-correlation was carried out between target stars and reference stars of similar spectral types. We present our measurements as a function of heliocentric Julian date in Table 3 where the template star used for each program star is indicated. Given the uncertainties in our measurements we will adopt an interval of  $\pm 20\text{ km s}^{-1}$  around the mean radial velocity of the cluster as a plausible range for inferring the membership of our candidates. In this respect, and averaging the various measurements available for some stars, we cannot exclude any of the four photometric candidates as likely members of the Coma cluster.

In addition to photometry, spectral type and radial velocity not inconsistent with being cluster members, the stars #1a, #2a, #3 and #7 show  $H\alpha$  in emission with equivalent widths (EWs) of few Angstroms. The  $H\alpha$  EWs that we measure from our spectra are tabulated in Table 2. All these four objects have emissions in agreement with their nature of X-ray emitters and with the status of members of the Coma star cluster. However, this property is neither a necessary nor a sufficient condition, since active field dMe stars also display  $H\alpha$  in emission, while a fraction of M dwarfs in the Hyades and Praesepe have  $H\alpha$  absorption (or very

**Table 3.** Radial velocities for the stellar X-ray candidates.

#	HJD (−2450520)	$v_{\text{rad}}^*$ (km s <sup>−1</sup> )	Template
1a**	–	−71... +43	BD+17 2785
2a	2.54759	+7	BD+17 2785
	2.56938	−9	
	2.59060	−22	
	3.54310	+23	
	3.56440	+38	
2b	2.54759	+60	BD+17 2785
	2.56938	+48	
	2.59060	+42	
	3.54310	+102	
	3.56440	+87	
3	2.75658	+4	BD+17 2785
	3.69987	+26	
4	2.01158	−65	HD 107513
	2.48902	−62	
	3.45152	+52	
5	2.68145	−20	HD 107513
	3.47941	−4	
7	3.68228	+4	BD+17 2785
8	2.70554	−18	HD 107513
	3.46854	−15	
10	2.50906	−5	BD+17 2785
	2.52275	−12	
	3.52481	+11	
11	2.65366	−14	BD+17 2785
	2.66634	−12	
	3.49793	+48	
12	2.49493	−22	HD 107513
	2.50199	−21	
	3.45803	+19	

\* Typical uncertainty is  $\pm 15$  km s<sup>−1</sup>.

\*\* The complete list of radial velocity measurements for this star is provided in Table 5.

weak emission; e.g., Barrado y Navascués et al. 1998; Stauffer et al. 1997). None of our targets has been observed to show flares.

### 3.3. Proper motions

We have successfully obtained proper motion measurements for those targets for which there is a spectroscopic and/or photometric suspicion of membership in the Coma cluster, i.e. stars #1a–c, #2a, #3 and #7. Because they are bright sources, all the candidates are well detected in the two epochs of observations of the Palomar Observatory survey. We have digitized an area of  $8' \times 8'$  of the Palomar plates centered at the coordinates of each of the program stars, and compared them to our IAC80 images. They are separated in time by 35.8 yr (Palomar epoch 1 and epoch 2) and 41.8 yr (Palomar epoch 1 and IAC80 data).

**Table 4.** Proper motion measurements.

#	$\mu_{\alpha \cos \delta}$ ("/yr)	$\mu_{\delta}$ ("/yr)
1a*	$-0.106 \pm 0.008$	$+0.014 \pm 0.006$
1b*	$-0.099 \pm 0.008$	$+0.014 \pm 0.006$
1c	$-0.053 \pm 0.008$	$+0.025 \pm 0.006$
2a	$+0.107 \pm 0.011$	$-0.063 \pm 0.012$
3	$-0.103 \pm 0.009$	$-0.052 \pm 0.012$
7	$-0.174 \pm 0.016$	$-0.019 \pm 0.010$

\* These two stars share the same proper motion.

This time baseline is enough for detecting an apparent motion of the cluster in comparison to the surrounding field stars. The mean proper motion of the Coma Berenices cluster is  $\mu_{\alpha \cos \delta} = -0.0123 \pm 0.0054''/\text{yr}$ ,  $\mu_{\delta} = -0.0097 \pm 0.0063''/\text{yr}$  ( $3\sigma$  uncertainties). These numbers result from the average of 35 Trumpler's (1938) cluster member proper motion determinations available in the catalogue by Abad & Vicente (1999). None of our candidates is, however, included in that work. Unfortunately, the cluster motion is not large and high precision measurements are needed in order to assess cluster membership. Nevertheless, if we find that our stars present a proper motion in disagreement with that of the Coma stellar group, we can reasonably claim that the candidates do not belong to Coma Berenices. The astrometric procedures we have used for deriving proper motions are simple: we derived  $x, y$  centroids for all stellar-like objects with S/N peak-detections larger than 5 in the images, and we proceeded to correlate their relative positions from the first epoch to the second and third epochs. Those objects with no apparent displacement were used to define the origin, and the movement of mobiles was then referred to them. Table 4 lists our final measurements together with  $1\sigma$  error bars. None of our five objects shows a stellar motion compatible with cluster membership; all of them move several times faster, and in some cases, the movement is in an opposite direction. Regarding the remaining X-ray candidates in our sample we have not detected significant motions in the time interval of our analysis.

One interesting by-product from the proper motion study is that stars #1a (RXJ 1212.0+2232) and #1b share the same motion in the sky within  $1\sigma$  uncertainty. This suggests that the two stars are real physical companions. Their photometry is also consistent with this result; the sequence defined by #1a and #1b nicely fits that of the main sequence shifted to a distance of 80–110 pc. The angular separation of the secondary star with respect the primary star is  $13''.1$  W and  $61''.9$  S (see Fig. 2); adopting the previous estimate of distance, this separation translates into 5000–7000 AU. From the photometric measurements of the fainter companion we can estimate its spectral type around M1–M3-class.

### 3.4. The W-type WUMa binary RXJ 1212.0+2232

From the photometric observations we have discovered one eclipsing binary star in our sample. More than 400 measures

**Table 5.** RXJ 1212.0+2232 radial velocity, H $\alpha$ , and S index measurements.

HJD (-2450520)	Phase	$v_{\text{rad}}^*$ (km s $^{-1}$ )	EW** H $\alpha$ ( $\text{\AA}$ )	S***
2.47238	0.25	-58	-	2.31
2.47743	0.27	-61	-	2.30
2.53724	0.54	-8	-	2.41
2.61414	0.89	+22	-	2.31
2.69849	0.27	-71	-	2.26
2.75032	0.51	-2	-	2.16
3.44460	0.66	+42	-0.59	-
3.49288	0.88	+43	-0.82	-
3.51630	0.98	+13	-0.90	-
3.59720	0.35	-19	-0.71	-
3.67366	0.70	+38	-0.61	-
3.73048	0.95	+9	-0.75	-

\* Typical uncertainty is  $\pm 15$  km s $^{-1}$ .

\*\* Typical uncertainty is  $\pm 0.10$   $\text{\AA}$ .

\*\*\* Typical uncertainty is  $\pm 0.30$ .

in the  $I$ -band are available for RXJ 1212.0+2232 (#1a) which have led to the determination of its orbital period. Periodogram analysis was performed on the differential photometry following the prescription of Scargle (1982) for unevenly sampled data. A significant peak (probability  $\sim 100\%$ ) was found at a period of  $5.2920 \pm 0.0001$  hr. Fig. 5 (upper panel) illustrates the light curve of RXJ 1212.0+2232 in the  $I$ -band folded in phase with the derived period and including all the data-points obtained at the two telescopes, IAC80 and OGS (different symbols are used). Individual photometric measurements of the OGS data for the two comparison stars present a scatter of about 0.006 mag, which is one order of magnitude smaller than the amplitude of modulation of RXJ 1212.0+2232, and do not show any correlation with phase. We do not tabulate individual measures in this paper, but will provide the data to anyone interested. The amplitude of the  $I$ -filter curve is determined at  $0.78 \pm 0.01$  mag; we cannot obtain the amplitude of the light curve at other wavelengths because of the lack of enough data. However, we have detected slight changes by 0.1 mag in the optical colours of this binary star as a function of the orbital phase. This could be related to the different temperature and mass of the two stellar components. We also note that around phase 0.25 (secondary maximum) the scatter in the magnitudes of the star is large. Such an effect is real and cannot be ascribed to poor photometric precision; it may be interpreted as a result of the different spot coverage in the stellar surfaces at the time of the observations. Twelve low-resolution spectra have been also obtained for this close binary. Double lines are barely resolved in some of them, and the cross-correlation technique used for deriving radial velocities is biased to the most intense lines. We provide our heliocentric radial velocity and H $\alpha$  EW measurements for one of the components of the system in Table 5; these values are given as a function of phase and heliocentric Julian date, and do correlate well with the light curve as it can be seen in Fig. 5 (lower panel).

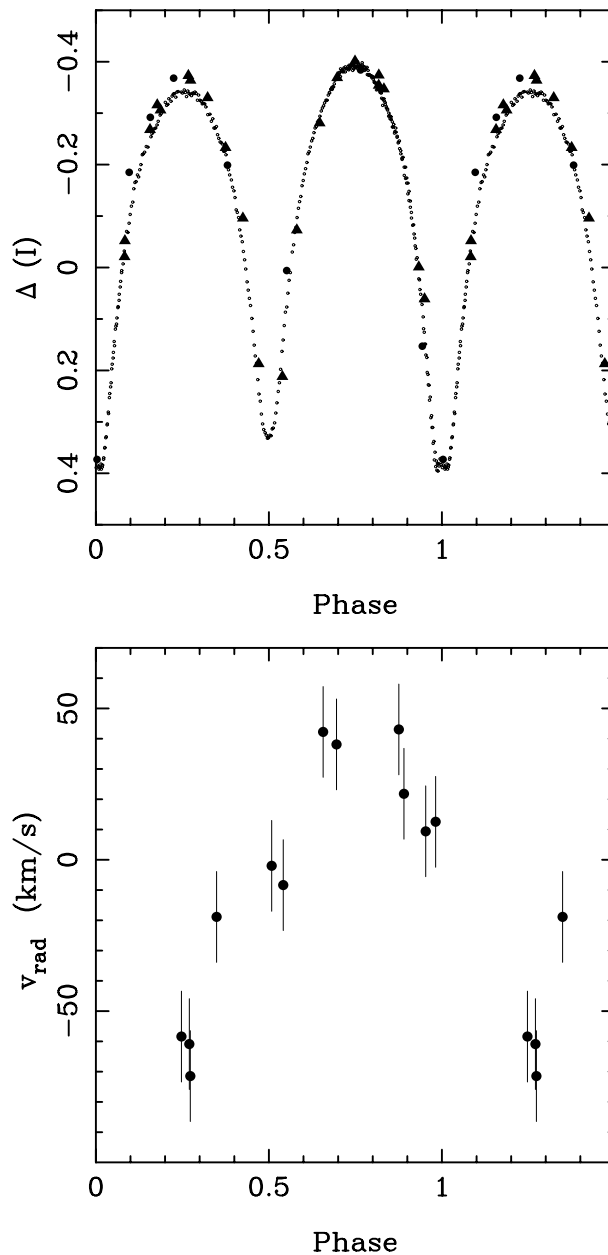


**Fig. 5.** (Upper panel). Phased  $I$ -band light curve for the star #1a (RXJ 1212.0+2232, K6V spectral type). Small dots correspond to the OGS observations (April 1999, uncertainties of 0.006 mag), while filled circles and triangles stand for the IAC80 data (February and March 1997, respectively). The period used is  $5.2920 \pm 0.0001$  hr. This light curve is typical of active W-type W UMa binaries. (Lower panel). Radial velocity measurements ( $1\sigma$  error bars) of one of the stellar components of the W UMa binary. The sinusoidal variation with phase is clearly seen.

The shape of the light curve of Fig. 5 corresponds to contact binary stars of the W UMa type. In the particular case of RXJ 1212.0+2232, the deeper light minimum results from the eclipse of the less massive (but hotter) component, implying that our star is a W-type W UMa binary system. This is also in accord with the late spectral type (K6V) of the source. We remark that

**Table 6.** Membership criteria.

#	Ph.	SpT	H $\alpha$	$v_{\text{rad}}$	PM	Final
1a	Y	Y	Y	Y	N	N
1b	Y?	–	–	–	N	N
1c	Y?	–	–	–	N	N
2a	N?	Y?	Y	Y	N	N
2b	N	N		N	N	N
3	N?	Y?	Y	Y?	N	N
4	N	N		N	–	N
5	N	N		Y	–	N
7	N?	Y?	Y	Y	N	N
8	N	N		Y?	–	N
10	N	N		Y	–	N
11	N	N		Y	–	N
12	N	N		Y	–	N

the period we have inferred for this contact binary star is among the shortest values found in the literature for this kind of stars. Although the frequency of the W UMa binaries is about one or two such systems per a thousand of ordinary dwarfs (Rucinski 1993), the discovery of RXJ 1212.0+2232 in our X-ray sample is not a surprise since W UMa stars are known to be strong X-ray emitters. Assuming a distance of 80–110 pc (see previous section) and the X-ray flux  $f_X = 4.01 \times 10^{-13} \text{ erg s}^{-1} \text{ cm}^{-2}$  given by RSP, we estimate for RXJ 1212.0+2232 an X-ray luminosity  $L_X = 3.0 - 5.8 \times 10^{29} \text{ erg s}^{-1}$ . Such a luminosity is consistent with those of known W UMa systems (e.g., McGale et al. 1996). In this kind of binary the stars are as close as double stars can be, sharing the same atmospheric envelope and showing the least amount of angular momentum among binary stars. We note that RXJ 1212.0+2232 is also a visual companion of a cooler star, forming a multiple stellar system. Only a few percent of these contact binaries are known to be visual companions.

## 4. Discussion

### 4.1. Cluster membership

Table 6 summarizes the criteria we have used in this paper in order to study the membership of our candidates in the Coma Berenices stellar cluster. These criteria are the following: (1) fitting the photometric and spectroscopic cluster sequence (Columns 2 and 3, respectively), (2) the presence of H $\alpha$  in emission and/or H $\alpha$  variability in the optical spectra (Column 4), (3) radial velocity consistent with the mean value of the cluster (Column 5), and (4) proper motion in agreement with the Coma star group (Column 6). We have assigned “Y” or “N” (followed by “?” in the case of marginal consistency) on the basis of what have been discussed in previous sections. The last criterion, proper motions, is the most decisive one when concluding on the membership status of our program stars.

As the table shows, *none* of the cluster X-ray candidates was confirmed as a cluster member by our analysis. This result contrasts with those for other clusters where, as mentioned in the Introduction, X-ray surveys and optical follow-up observations were instead very successful in identifying previously

unknown cluster members. This, in turn, suggests two possible conclusions: (1) since Coma is considerably older than the clusters where new members were identified through ROSAT surveys, its population of low mass stars, if existent, must be considerably X-ray fainter. Therefore, possible late-type cluster members may have not been detected (discovered) in X-rays because their X-ray luminosities are below the sensitivity of the RSP ROSAT observations; (2) alternatively, Coma sequence does really truncate at  $M_V \sim 6$ , at least in the cluster core which was covered by the X-ray survey. Since the XLDF of solar-type stars in the Hyades and Coma are very similar (the Coma population of solar-type stars actually appears slightly more X-ray active), we can make the plausible assumption that the same occurs for lower mass stars. Under this assumption, the sensitivity of the RPS X-ray survey should have allowed detecting part of these low mass stars; the fact that we do not detect them argues in favour of a drastically reduced population of low mass stars in Coma, consistently with the results of the optical surveys. Unfortunately, the limited cluster coverage of the X-ray survey, which did not extend much beyond the cluster core, does not allow us to say much about the existence (and the spatial distribution) of K/M dwarfs outside the cluster core and, in particular, about the existence of extratidal low mass stars.

### 4.2. Nature of the X-ray detected sources

Whereas our analysis indicated that the X-ray candidates are not cluster members, we believe that, on the basis of our photometric and spectroscopic data in the visible, the stars #1a, #2a, #3, #4, #7, #10, #11 and #12 can still be considered as the optical counterparts of the X-ray sources of Table 1 (RSP). These optical counterparts are located within a distance of 30'' from the X-ray coordinates. They comply with the expected properties of being late-type chromospherically active objects, showing H $\alpha$  emission for most of the late-K/M cases. Only the G-type stars #5 and #8 show a potentially low chromospheric activity. As it can be seen in the finding charts shown by RSP, there are two other non-stellar and fainter objects located close to the star #5, and the star #8 lies slightly further than 30'' from the corresponding X-ray coordinates. These facts could be related to the stars not being the optical counterparts of the X-ray sources.

RXJ 1212.0+2232 (#1a) has already been discussed in Sect. 3.4. We divide the remaining sources in two groups on the basis of their location on the colour-magnitude diagrams, namely, those lying above the Coma sequence (group a) and those lying below it (group b). If, as supported by the good matching between the colours and the spectral-types, the reddening towards these stars is negligible, stars in group a) are likely to be slightly closer to us than Coma. The absence of detectable lithium lines in the spectra of these late-type stars suggests that, if they are single objects, they could be as young as 50–70 Myr (a total Li preservation, which takes place until about 10–20 Myr, would have produced features clearly observable with our spectral resolution; Pavlenko et al. 1995). Therefore, these objects cannot be very young stars still above the main sequence and located beyond the Coma cluster. Further-

more, H $\alpha$  EWs of stars in group a) are comparable to those of Hyades stars with the same colours and/or to those of active field dMe dwarfs, and these stars show a very high level of chromospheric activity. Therefore, they are most probably “normal” foreground young-to-intermediate age M dwarfs.

Stars in group b), instead, should have larger distances than Coma. This sample is very probably constituted by a combination of rather young stars and active binaries. The radial velocities we infer, with changes in magnitude and sign, suggest that at least three of the objects in this group (#4, #11, and #12 –plus #2a in group a) could in fact be binary systems: these objects have radial velocity measurements diverging by more than  $3\sigma$  the error bar and thus could be rapid-rotating spectroscopic binaries (note that our spectral resolution is  $\sim 200$  and  $150 \text{ km s}^{-1}$  for the blue and red spectra, respectively). However, observations in the R-band performed to search for photometric variability of these stars on February 29, 2000 (using the IAC80 telescope and the instrumental setup described in Sect. 2.2), showed that there was no detectable variation within 0.05 mag for any of these objects. On the other hand, there is no indication of binarity for stars #5, #8, #10. Having only one red spectrum for the star #7 does not allow us to go further than providing its spectral type and radial velocity at the time of the observation. The lower limits to the X-ray luminosities that we derive for the two G-type stars, if they are the optical counterparts of the X-ray sources, are consistent with an age comparable to the Hyades or slightly younger; vice versa, both the lower limit to its X-ray luminosity and its H $\alpha$  EW suggest that star #10 should be at least as young as the Pleiades (120 Myr).

Our conclusion that this sample of stellar X-ray sources not belonging to Coma is composed by a mixture of young to intermediate-age stars and close active binaries is consistent with the results of the optical follow-up studies of Einstein and EXOSAT serendipitous sources (Favata et al. 1993; Tagliaferri et al. 1994). Furthermore, we have compared the number of detected stellar X-ray sources (including both the 10 objects from the present study and those already known in the SIMBAD database –see RPS) with the expected number based on the models of the distribution of X-ray sources in the Galaxy constructed by Guillout et al. (1996) and on the sensitivity of the RPS X-ray survey. We estimate that no more than one stellar X-ray source (not belonging to Coma) per square degree has been detected in the ROSAT survey and that the predicted number of stellar X-ray sources per square degree is of the order of 2. The sensitivity of the Coma X-ray survey is not uniform, which introduces additional uncertainties in our estimate. It is important, however, the fact that we detect *less* stellar X-ray sources than predicted and not *more*: this provides an additional support to the conclusion that the objects studied by us are not members of the Coma Berenices open cluster.

## 5. Conclusions

We have conducted a photometric and spectroscopic optical follow-up of 12 X-ray sources detected by ROSAT in the center field of the Coma Berenices open cluster. *VRI* colours, spectral

types, chromospheric activity and radial velocities were derived for all the stellar candidates observed. Four of these stars exhibit both photometric and spectroscopic properties which are marginally compatible with cluster membership. Their proper motions are, however, much higher than the cluster’s value, implying that they do not belong to it. We have discussed their probable nature on the basis of the available information, but higher resolution spectroscopy and photometric monitoring would be needed to better ascertain their stellar properties. Changes in radial velocities indicate that five of the stellar objects in the sample could be binaries, and one of them has turned out to be a K6 W-type W UMa contact binary exhibiting one of the shortest periods known for this kind of systems.

Coma Berenices appears then to be an open cluster with not enough mass to retain its less massive original stars. Additional X-ray/optical observations are needed to investigate the existence and distribution of late-type stars outside the cluster core.

*Acknowledgements.* We thank I. García de la Rosa for his assistance with the observations of the second campaign at the IAC80 telescope, and the referee, Dr. G.R. Knapp, for her comments.

This research has made use of the SIMBAD–CDS database, and was partially supported by the Spanish DGES under projects PB95-1132-C02-01 and PB98-0531-C02-02. SR and RP acknowledge the financial support of the Italian Ministry of University, Scientific Research and Technology (MURST) through the grant Cofin98-02-29.

## References

- Abad C., Vicente B., 1999, A&AS 136, 307
- Alonso A., Arribas S., Martínez-Roger C., 1995, A&A 297, 197
- Alonso A., Arribas S., Martínez-Roger C., 1996, A&A 313, 873
- Argue A.N., Kenworthy C.M., 1969, MNRAS 146, 479
- Artyukhina N.M., 1955, Trudy gos. astr. Inst. Sternberga 26, 3
- Bade N., Engels D., Voges W., et al., 1998, A&AS 127, 145
- Barrado y Navascués D., Stauffer J.R., Randich S., 1998, ApJ 560, 347
- Barry D.C., 1988, ApJ 334, 436
- Bounatiro L., 1993, A&AS 100, 531
- D’Antona F., Mazzitelli I., 1998, <http://www.mporzio.astro.it/~dantona/index.html>
- De Luca E.E., Weis E.W., 1981, PASP 93, 32
- Dufflot M., Figon P., Meyssonnier N., 1995, A&AS 114, 269
- Duncan D.K., Vaughan A.H., Wilson O.C., et al., 1991, ApJS 76, 383
- Favata F., Barbera M., Micela G., Sciortino S., 1993, A&A 277, 428
- García López R.J., Rebolo R., Beckman J.E., McKeith C.D., 1993, A&A 273, 482
- Guillout P., Haywood M., Motch C., Robin A.C., 1996, A&A 316, 89
- Jaschek M., 1978, Bull. Inform. CDS 15, 121
- Jeffries R.J., 1999, In: Butler C.J., Doyle J.G. (eds.) Solar and Stellar Activity: Similarities and Differences. A conference dedicated to Brendan Byrne. ASP Conference Series 158, p. 75
- Johnson H.L., Knuckles C.F., 1955, ApJ 122, 209
- Kirkpatrick J.D., Henry T.J., McCarthy D.W. Jr., 1991, ApJS 77, 417
- Landolt A.U., 1992, AJ 104, 340
- Leggett S.K., Allard F., Berriman G., Dahn C.C., Hauschildt P.H., 1996, ApJS 104, 117
- McGale P.A., Pye J.P., Hodgkin S.T., 1996, MNRAS 280, 627
- Mendoza E.E., 1963, Bol. Obs. Tonantzintla y Tacubaya 3, 137

- Montes D., Martín E.L., Fernández-Figueroa M.J., Cornide M., De Castro E., 1997, *A&AS* 123, 473
- Noyes R.W., Hartmann L.W., Baliunas S.L., Duncan D.K., Vaughan A.H., 1984, *ApJ* 279, 763
- Odenkirchen M., Soubiran C., Colin J., 1998, *New Astr.* 3, 583
- Oke J.B., 1990, *AJ* 99, 1621
- Pavlenko Ya.V., Rebolo R., Martín E.L., García López R.J., 1995, *A&A* 303, 807
- Pickles A.J., 1985, *ApJS* 59, 33
- Prosser C.F., Randich S., 1998, *Astron. Nachr.* 319, 201
- Prosser C.F., Stauffer J.R., Kraft R.P., 1991, *AJ* 101, 1361
- Prosser C.F., Stauffer J.R., Caillault J.-P., et al., 1996, *AJ* 110, 1229
- Pye J.P., Hodgkin S.T., Stern R.A., Stauffer J.R., 1994, *MNRAS* 266, 798
- Randich S., 1997, *Mem. Soc. Astron. Ital.* 68, 971
- Randich S. 2000, In: Pallavicini R., Micela G., Sciortino S. (eds.) *Stellar Clusters and Associations: Convection, Rotation, and Dynamos*. ASP Conference Series, in press
- Randich S., Schmitt J.H.M.M., Prosser C.F., Stauffer J.R., 1995, *A&A* 300, 134
- Randich S., Schmitt J.H.M.M., Prosser C.F., 1996a, In: Zimmerman, H.U., Trümper J., Yorke H. (eds.) *Proc. Röntgenstrahlung from the Universe*. MPE Report 263, p. 61
- Randich S., Schmitt J.H.M.M., Prosser C.F., 1996b, *A&A* 313, 815
- Rucinski S.M., 1993, In: Sahade J., Kondo Y., McClusky G. (eds.) *The Realm of Interacting Binary Stars*. Kluwer, Dordrecht, p. 111
- Rutten R.G.M., 1987, *A&A* 177, 131
- Scargle J.D., 1982, *ApJ* 263, 835
- Schrijver C.J., Dobson A.K., Radick R.R., 1989, *ApJ* 341, 1035
- Stauffer J.R., Hartmann L.W., Prosser C.F., et al., 1997, *ApJ* 479, 776
- Tagliaferri G., Cutispoto G., Pallavicini R., Randich S., Pasquini L., 1994, *A&A* 285, 272
- Trumpler F.J., 1938, *Lick Obs. Bull.* 18, 167
- Van Leeuwen F., 1999, *A&A* 341, L71
- Vaughan A.H., Preston G.W., 1980, *PASP* 92, 385
- Vaughan A.H., Preston G.W., Wilson O.C., 1978, *PASP* 90, 267
- Walter F.M., 1982, *ApJ* 253, 745
- Woolley R.v.d.R., Epps E.A., Penston M.J., Pocock S.B., 1970, *Royal Obs. Ann* 5, 1